Institute of Paper Science and Technology
500 10th Street, NW
Atlanta, GA 30318

Kinetics of Ba(OH)$_2$ Reaction with Na$_2$CO$_3$ and Na$_2$SO$_4$
&
Particle Separation Characteristics from White Liquor

6190 Research Project

by
Alexander L. Quesada
Candidate for Master's Degree

Submitted to
The Academic Office
April 16, 2003

Advisor:

Howard (Jeff) L. Empie

Table of Contents

1. Abstract

The purpose of this study is to determining the feasibility of replacing causticizing (calcium based reactions and precipitate) with bausticizing (barium based reactions and precipitates). Bausticizing is not limited by chemical equilibrium and thus can proceed to full conversion eliminating the dead load of inert sodium carbonate in the white liquor. The comparison is centered on the kinetics and conversion as well as precipitate sedimentation.

$BaCO_3$ and $BaSO_4$ approach full conversion (97.7% and 95.9% respectively) after a 5 to 10 second reaction at room temperature with 0.1M feed solutions ($Ba(OH)_2$, Na_2CO_3, and Na_2SO_4). Barium mud settling behavior is comparable to that of lime mud and can possibly be carried out by existing sedimentation tanks within a pulp mill.

2. List of Tables and Figures

3. Project Introduction and Background

The traditional chemical recovery cycle (Figure 1) employs a causticizing reaction, using calcium hydroxide, $Ca(OH)_2$, to react with sodium carbonate, Na_2CO_3, for regenerating an active white liquor compound, sodium hydroxide (eq. 2).

$$CaO_{(s)} + H_2O \rightarrow Ca(OH)_2 + heat \qquad \text{(eq. 1)}$$

$$Na_2CO_{3(aq)} + Ca(OH)_{2(s)} \Leftrightarrow 2NaOH_{(aq)} + CaCO_{3(s)} \qquad \text{(eq. 2)}$$

$$CaCO_{3(s)} + heat \rightarrow CaO_{(s)} + CO_{2(g)} \qquad \text{(eq. 3)}$$
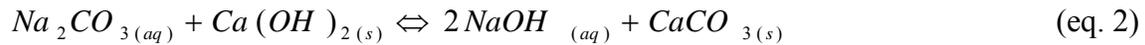
Sodium sulfide, Na_2S, is also an active white liquor compound and thus introduces the sulfur element to the pulping and recovery processes.

$$Na_2S_{(aq)} + H_2O_{(aq)} \Leftrightarrow NaOH_{(aq)} + NaHS_{(aq)} \qquad \text{(eq. 4)}$$

After white liquor is consumed in the pulping process, the black liquor by-product, containing dissolved organics and inorganics, is burned in the recovery furnace for steam production. The recovery furnace is responsible for producing the desired Na_2S in a reducing environment where sub-stoichiometric oxygen is added to minimize oxidation of sulfur. The combustion of black liquor in the recovery furnace will convert the sodium and sulfur compounds to Na_2CO_3 and a mixture of Na_2S and Na_2SO_4 [1]. These sodium compounds make up the molten smelt, which dissolves in a tank to produce green liquor. Green liquor is then used to dissolve reburned lime in the slaker (eq. 1). The completion of the process is then carried out in the causticizers. The $CaCO_3$ formed in the reaction is then regenerated to CaO in the calcination reaction which simply breaks down $CaCO_3$ at about 800°C (eq. 3).

The causicizing reaction (eq. 2) is governed by equilibrium, therefore, not all the Na_2CO_3 is converted to the desired product, NaOH. The extent to which the reaction is carried to completion is known as causticizing efficiency. A high percentage conversion is desirable to reduce the loading of inert Na_2CO_3 in the recovery cycle [2]. A typical causticizing efficiency is about 80%. This, in effect, constitutes a dead load of about 18 % by weight (solids basis) of the inactive white liquor component, Na_2CO_3. The Na_2SO_4 contributes a dead load of about 4 % by weight (solids), which circulates through the process due to the limit of reduction efficiency (typically greater than 90%) in the recovery furnace. The combined dead load of Na_2CO_3 and Na_2SO_4 occupies reactor space and consumes energy, therefore, costing pulp mills money.
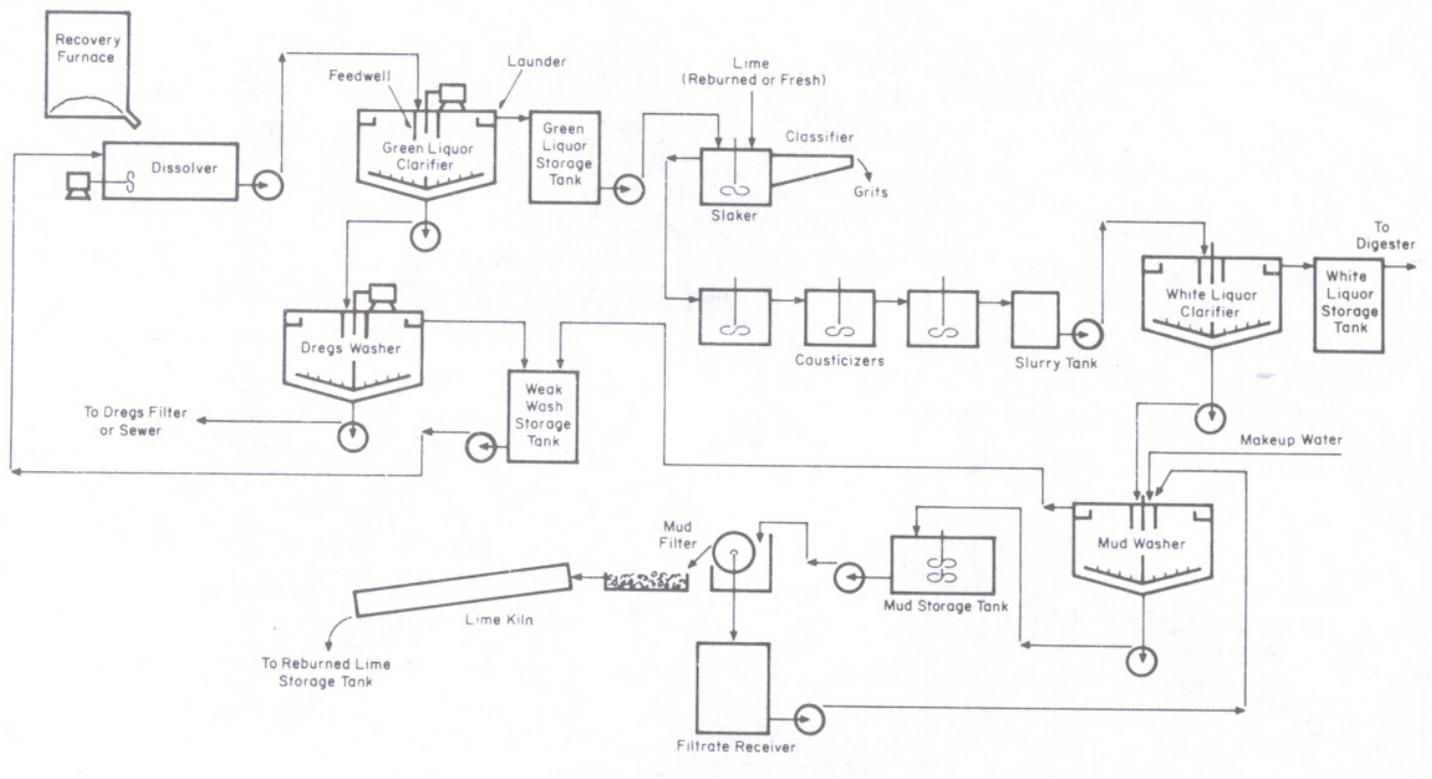
Figure 1. Recovery Cycle Process Flow Diagram [2].

An alternative causticizing agent is proposed: Barium Hydroxide, $Ba(OH)_2$. This reagent is valuable because the barium salts produced ($BaCO_3$, $BaSO_4$) are insoluble. Without chemical equilibrium limitations, the reactions proceed to completion without a possible reverse reaction. This new causticizing process could thus be called "bausticizing."

The purpose of this project is to determine the feasibility of bausticizing.

$$Na_2CO_{3(aq)} + Ba(OH)_{2(aq)} \rightarrow 2\,NaOH_{(aq)} + BaCO_{3(s)} \qquad \text{(eq. 5)}$$

$$Na_2SO_{4(aq)} + Ba(OH)_{2(aq)} \rightarrow 2\,NaOH_{(aq)} + BaSO_{4(s)} \qquad \text{(eq. 6)}$$
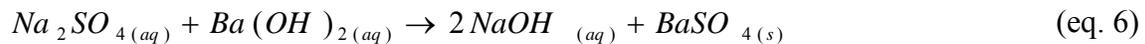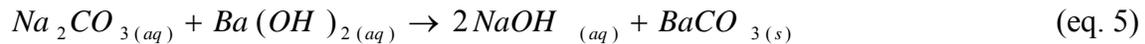
The corresponding regeneration reactions, to be done in a kiln or fluidized bed, *not* addressed in this study, are:

$$BaCO_{3(s)} + heat \rightarrow BaO_{(s)} + CO_{2(g)} \qquad \text{(eq. 7)}$$

$$Ba_2SO_{4(s)} + 2C \rightarrow BaS_{(s)} + 2CO_{2(g)} \qquad \text{(eq. 8)}$$

The second part of this project is to evaluate the sedimentation behavior of the new barium mud that will be formed by bausticizing. The data can then be compared to that of lime mud formed by causticizing to determine if the barium based solid-liquid separation can be carried out with existing sedimentation tanks in a typical pulp mill.

4. Literature Review

4.1 Kinetics

The literature has indicated that kinetics for the proposed bausticizing reactions (eq. 5 & 6) are extremely fast and difficult to analyze with accuracy.

A review of past research performed with the reaction of $Ba(OH)_2$ and Na_2CO_3 to form the precipitated $BaCO_3$ shows a proposed nucleation and crystal growth rate expression derived from the work done by Salvatori [3]. The goal of his research was to simulate operating conditions encountered in industrial processes with high pH and high reagent concentrations. These conditions will also be encountered if bausticizing is determined to be feasible in replacing in the traditional causticizing reaction for making white liquor. The result from his work, showing a primary heterogeneous mechanism, is displayed below:

$$r_N = A_0 e^{-E/RT} e^{-B/(\ln S)^2} \qquad \text{(eq. 9)}$$

Where $A_0 = 6.4 \times 10^{24}$ $m^{-3}s^{-1}$, E = 22065 J/mol, B = 58.7, and S is the supersaturation ratio varying from 35 to 280.

Apparently the expression above can calculate the nucleation rate with an uncertainty of about 50% which, Salvatori claims, is very satisfactory for this kind of measurement.

An explicit expression for measuring the nucleation rate for $BaSO_4$ was not obtained from literature.

4.2 Particle Size, Agglomeration, Crystal Morphology, and Aging

A review of research performed by Dorris [4] on the lime mud ($CaCO_3$) particles shows that very little data have been published on the size distribution of lime mud particles associated with the causticizing reaction in the pulp and paper industry.

Particle size measurements are sometimes not really measurements of actual nucleated particles, but rather measurements of the network of associated particles forming larger agglomerates or aggregates. The terms "agglomerates" and "aggregates" are analogous, but Dorris uses aggregates to describe coagulated particles of primary agglomerates during lime mud sedimentation.

Some data taken from mud filters of different mills indicate an agglomerate volume diameter from 9 to 26 μm and a lime mud aggregate range from 68 to 132 μm, results of which suggest that different operating conditions can yield different particle sizes and aggregates.

Sources have indicated that $BaCO_3$ particles behave similarly to $CaCO_3$ particles in agglomeration behavior [5, 6]. Two sources have suggested that $BaSO_4$ particles do not agglomerate, at least not to the extent that $BaCO_3$ does [6, 7].

A study on crystal morphology of $BaCO_3$ particles has been performed by Chen [5]. This study shows that different types of crystals can be formed by controlling the pH, ionic strength, and initial concentrations. Some of the different types of crystals encountered in Chen's research are displayed below in Figure 2.
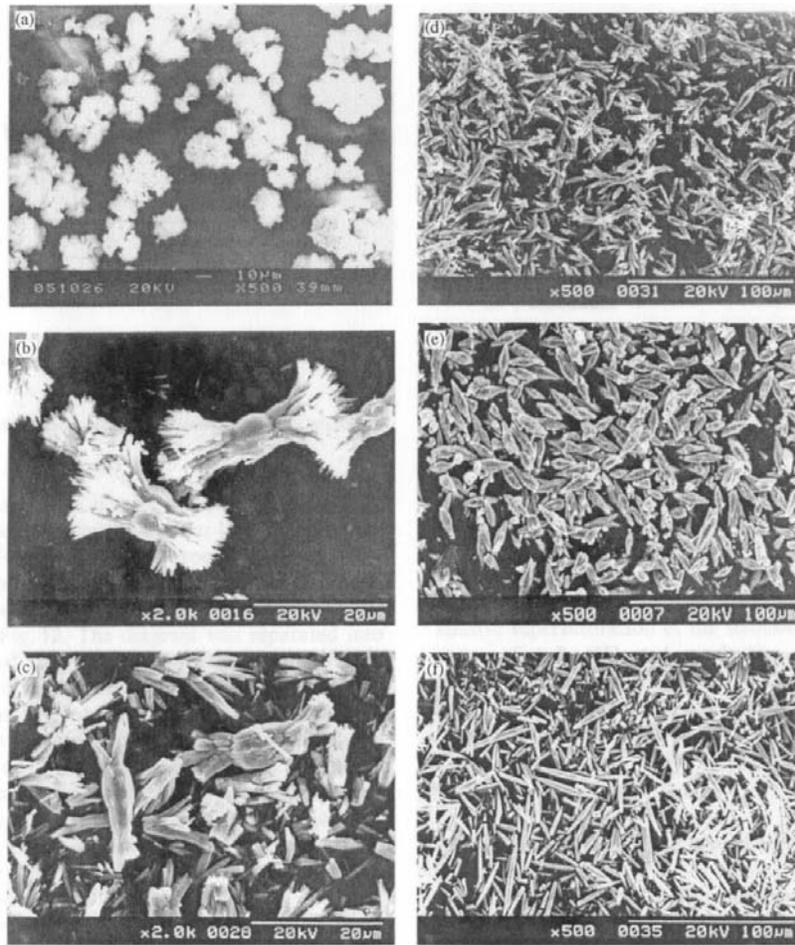
Figure 2. Morphology of barium carbonate crystals: (a) floc crystals, (b) candy-like crystals, (c) olivary with end dendrite crystals, (d) olivary with end dendrite crystals, (e) olivary-like crystals, (f) needle-like crystals.

The crystals in Chen's research were formed under controlled conditions "not akin" to heavy industrial processes as described earlier in this report. The results are still valuable in exploring the possible effects of crystal morphology on the structure and properties of agglomerates which will certainly affect the particle settling rate.

Another topic explored in the literature review is the poorly known complex theory of aging. Aging is the process by which the physical characteristics of solids, such as crystals, can change due to the following processes as described by Rousseaux [8]: "(a) recrystallization of the primary particles into more compact shapes through surface diffusion of mass transport through the liquid phase; (b) transformation of metastable crystal modifications into stable modifications by dissolution and recrystallization: (c) aggregation of primary particle and subsequent intergrowth; and (d) growth of larger particles at the expense of smaller particles." Since aging is most important for poorly soluble substances like that of $BaCO_3$ and $BaSO_4$, the aging theory will be considered if changes in crystal appearance and/or settling behavior over time occur with the barium salts.

4.3 Settling Rate and Mud Solids Concentration

Currently, white liquor is clarified by using the settling properties of lime mud ($CaCO_3$), including density, particle structure, and at times electrical potential or zeta potential. Typically lime mud is separated from white liquor in large gravity sedimentation tanks (Figure 3) where the concentration of lime mud feed lies between 80 to 125 kg/m^3 as stated in Dorris's work. The respective lime mud solids concentration in the underflow or settled region is between 35% and 40% solids by weight [9].
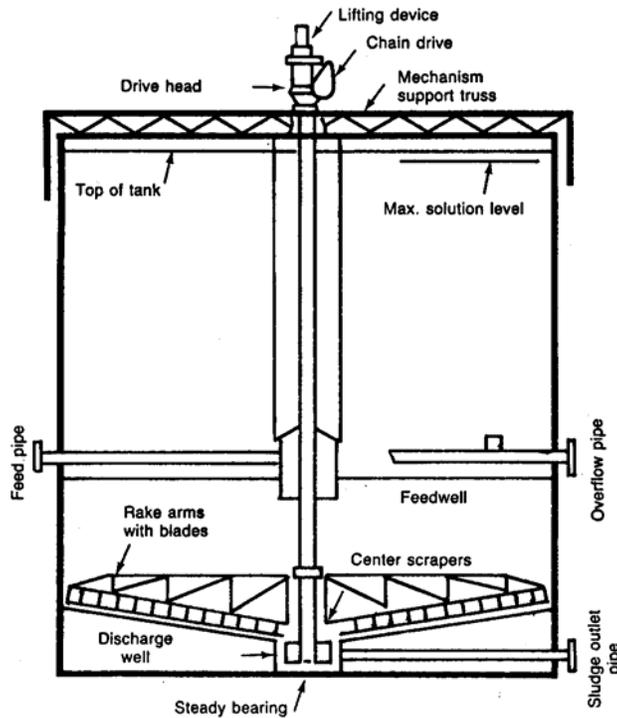
Figure 3. Typical white liquor clarifier [9].

Lime mud settling is classified as hindered settling by the gravitational settling phenomena described in the textbook, Wastewater Engineering [10]. A schematic for a typical settling curve describing the different settling regions is displayed in Figure 4.

In systems which contain a high concentration of suspended solids (i.e., lime mud sedimentation) both hindered settling regions and compression regions are present along with the discrete and flocculant settling regions. An interface usually occurs between the hindered settling region and the relatively clear upper regions. This interface is measured with respect to time to determine sedimentation behavior of the solids under consideration.
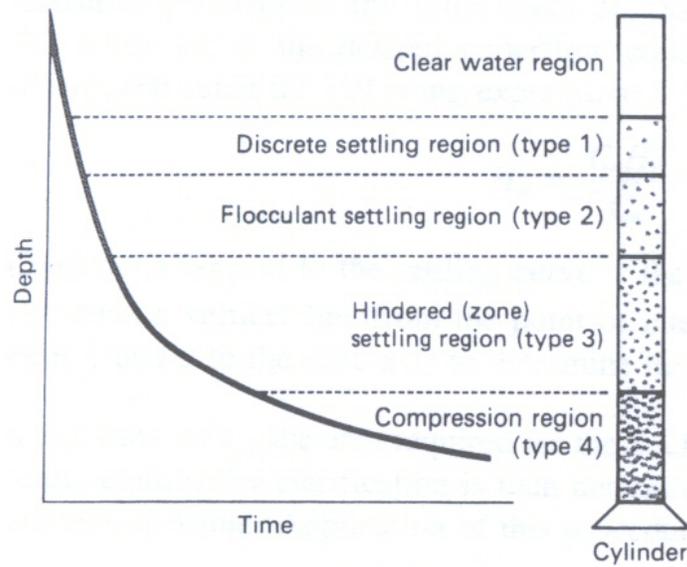
Figure 4. Settling regions representative of lime mud settling behavior [10].

An expression for terminal settling velocity that can be used as a tool to find optimum conditions for settling is expressed in the equation below. This relation is only valid to estimate settling velocity in the discrete settling region or flocculant settling region as described in Figure 4.

$$u = \frac{gd^2(\rho_p - \rho_l)}{18\mu} \qquad \text{Re}_p < 0.1 \qquad \text{(eq. 10)}$$

Where: u = terminal velocity g = acceleration due to gravity

ρ_p = particle density d_p = particle diameter

ρ_l = fluid density μ = fluid viscosity

Terminal settling velocity equation taken from Perry's Chemical Engineer Handbook [11].

5. Present Study

The primary purpose of this project is to show whether the proposed bausticizing reactions are capable of replacing the current causticizing reactions due to better kinetic performance and increased conversion, thereby, eliminating reactor space and dead load.

Studying the settling behavior of the precipitated barium salts is also important to determine whether existing clarification equipment in pulp mills is capable of carrying out the solid-liquid separation that is required, or that an alternative method will be needed.

5.1 Experimental Design (Kinetics & Conversion)

The experiment was originally designed to determine a kinetic rate law using elementary reaction kinetics where the rate equation corresponds to the simplified homogeneous stoichiometric equation:

Stoichiometric equation: $$aA + bB \rightarrow products \qquad (eq. 11)$$
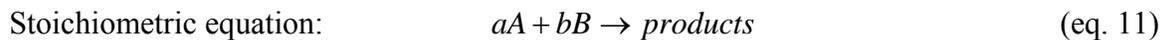
Rate equation: $$-r_A = -\frac{dC_A}{dt} = kC_A{}^a C_B{}^b \qquad (eq. 12)$$

Stoichiometric coefficients are represented by a & b. Stoichiometric coefficients determine the reaction order by addition.

Based on the Arrhenius Law, the rate constant (k) can be related to temperature (T) by the following equation, where R is the molar gas constant and E is the activation energy [12].

Arrhenius equation: $$k = k_0 e^{-E/RT} \qquad (eq. 13)$$

This method proved to be experimentally unfeasible due to the instantaneous nature of the bausticizing reactions.

A more qualitative approach was instituted, whereby the conversion after about 5 seconds was determined at room temperature.

5.2 Experimental Procedure (Kinetics and Conversion)

Equal molar (0.1M) mixtures of 100 ml of Na_2CO_3 and 100 ml of Na_2SO_4 were each reacted separately at room temperature (25°C) with 100 ml of 0.1M $Ba(OH)_2$. The products were allowed to react for about 5 seconds then quickly quenched with 500 ml of 5°C water. The precipitate was then filtered through filter paper and oven dried to calculate conversion.

5.3 Experimental Procedure (Particle Size)

The particle size analysis was performed by using a Malvern Particle Size Analyzer. A sample of the precipitated salts were feed into a small stir tank which circulated the solution to the device which employed a laser for light scattering diffraction analysis to obtain a particle size distribution.

5.4 Experimental Procedure (Sedimentation)

A 100 ml graduated cylinder was used to determine the settling curves for the precipitated barium salts. The height of the graduated cylinder was 18.9 cm. This will represent H_0 for the settling curve. Each hash mark on the 100 ml cylinder thus represents 18.9/100 cm. Settling height interface vs. time data were then gathered for the various reaction conditions. Settling curves were compared using equal volumetric portions of precipitated solids. Due to the small size of the graduated cylinder, a volume of 0.15 cm^3 was used. The mass required was based on the specific gravity. See Table 1.

Table 1. Precipitate Comparison

	Causticizing	Bausticizing	
Precipitate	$CaCO_3$	$BaCO_3$	$BaSO_4$
Specific Gravity	2.8	4.3	4.5

6. Results and Discussion

6.1 Kinetics and Conversion

The conversion data for the bausticizing reactions performed in a reaction time of about 5 seconds are displayed in Table 2.

Table 2. Conversion Data*

Precipitate	Conversion	Stdev
$BaCO_3$	97.7%	0.01
$BaSO_4$	95.9%	0.04

*Six tests performed for each precipitate

It's safe to assume from basic kinetic rate laws, that if a reaction is essentially instantaneous at 25°C, then it will surely be faster at higher temperatures, especially those encountered in the causticizing processes (80-90°C). The cold water quench was unnecessary due to the fast conversion. The possible experimental error limiting the conversion to 97.7% and 95.9% can be attributed to precipitate lost through the filtering process. It is plain to see that bausticizing reactions have a great advantage over that of causticizing due to the essentially full conversion, as well as rapid reaction kinetics.

6.2 Particle Size Analysis

The particle size measurements taken from the Malvern Particle Size analyzer were used to hone in on the average agglomerate size. The intended purpose, however, proved unreliable for accurate results. This study did not determine the extent to which agglomerates are broken during the mixing and circulation of the slurry in the stir tank of the particle size analyzer. Also, particle size measurements can vary for the same sample due to inconsistent obscuration levels in the fluid moving across the laser. No extensive investigation on the accuracy of the size analyzer was performed. Despite these minor uncertainties, the particle size analyzer was still a valuable tool in gathering information on trends that were discovered dealing with the average particle size of barium carbonate vs. time. See Table 3.

Table 3. Barium Carbonate Particle Size (microns)

Day	Sample 1	Sample 2	Sample 3	Sample 4
0	31	33	32	25
1	23	20		
7	10	12	12	14

The particle size of $BaCO_3$ decreases with age. This trend may be explained by one or more of the aging theories proposed in the literature. $BaCO_3$ particles were also noticeably different with the naked eye. When first reacted at 25°C, the precipitate is snowflake-like and fluffy in appearance, likely containing a significant amount of occluded or trapped water. After aging the precipitate for 7 days, it becomes more compact, and less fluffy in appearance, likely increasing the overall specific gravity of the agglomerated particle. It will become interesting to note the possible aging effect of $BaCO_3$ when studying the settling curves.

BaSO$_4$ particles do not display this kind of trend which may support the observation that BaSO$_4$ particles do not agglomerate or even age to the same extent that BaCO$_3$ particles do. In fact BaSO$_4$ particles measured consistently at about 7 microns.

6.3 Sedimentation for Barium Salts

The peculiar change in particle size due to some unknown aging process also appears to affect the settling rate of BaCO$_3$. The first of these observances is displayed in Figure 5, showing the height of the sedimentation bed interface (with the clear water region above) vs. time.
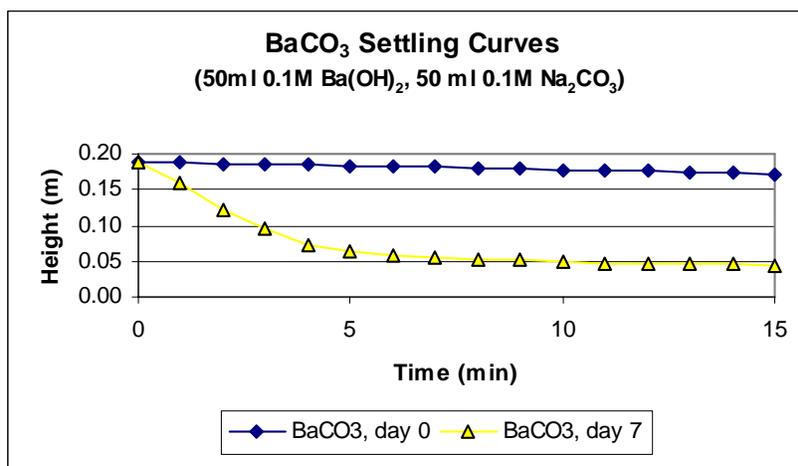
Figure 5. Aging effect of BaCO$_3$.

The settling curve has changed dramatically simply by aging BaCO$_3$ seven days. The first curve (day 0) hardly changes over the 15 minute observation. The particles in the slurry appear to be locked in a suspension or network-like structure throughout the cylinder. The particles are light, fluffy, and snowflake like in appearance. The settling behavior mimics that of the hindered or compression regions as described in Section 4.3.

The second curve (day 7) shows the transition from the discrete settling region to the compression region. The particles are noticeably more aggregated or compact and less fluffy in appearance.

The next experiment in this study is to see what effect temperature has on the settling behavior. This experiment was performed using two conditions for precipitation:

(1) Heat reactants to 80°C. Then react to form precipitate and pour slurry into graduated cylinder.

(2) React solutions at 25°C to form precipitate. Then heat slurry to 80°C and pour into graduated cylinder.

Note: Solutions or slurries take several minutes (1-3 min) to heat to 80°C. The precipitated slurry is then free to cool at room temperature during the sedimentation process. The precipitated slurries cooled from 80°C to an average temperature of about 54°C.

Results from the two reaction conditions and aging are displayed in Figure 6.

BaCO₃ Settling Curves
(33ml 0.1M Ba(OH)₂, 67 ml 0.1M Na₂CO₃)
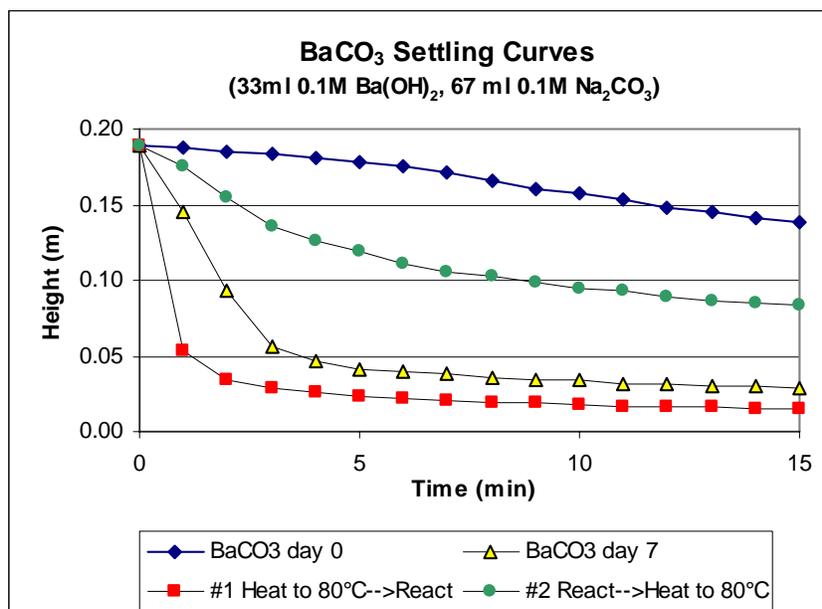
Figure 6. Two reaction conditions and aging of $BaCO_3$.

The settling curves for the two reaction conditions are quite different. Reaction at 80°C gives the best settling performance. Heating a mixture, precipitated at room temperature,

to 80°C simply increases the settling rate.   Performing the precipitation reaction at 80°C prior to sedimentation increases the settling performance even more.

The viscosity of water decreases with temperature increase. In fact the viscosity drops from 1 centipoise at 20°C to 0.35 centipoise at 80°C.   An increase in temperature will help the water move more easily through the interstices of the settling precipitate, thus decreasing the volume of water trapped in the void space during compression.

This viscosity change of water, however, does not explain why reacting at a higher temperature improves the sedimentation. Perhaps different types of crystals are formed yielding agglomerates of higher density. Or perhaps there is a fundamental change in the crystal structure or change in the network of agglomerates that can only be explained by aging phenomena.

The next experiment explores the settling behavior after cooling the two product slurries, from the two reaction conditions performed, to 10°C. See Figure 7.

BaCO₃ Settling Curves
(33ml 0.1M Ba(OH)₂, 67 ml 0.1M Na₂CO₃)
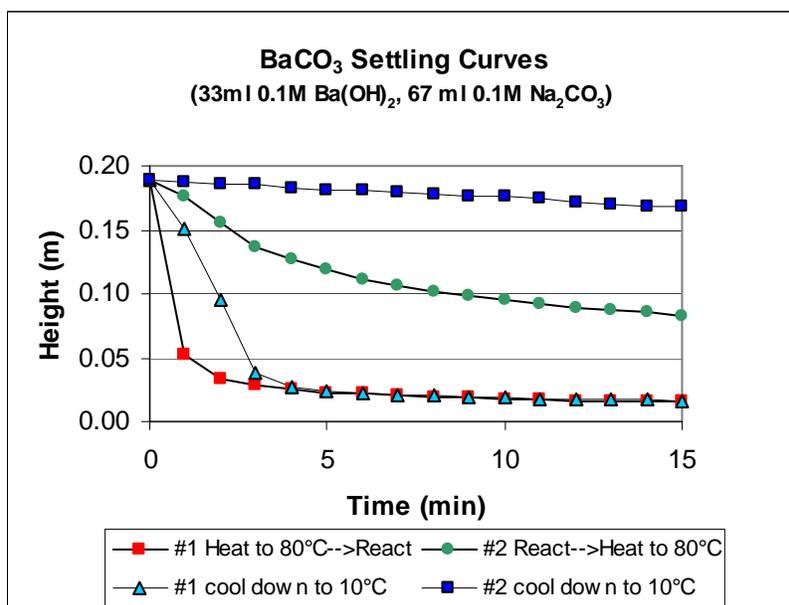
Figure 7. Cooling effect on BaCO₃ sedimentation.

The data above show for the first reaction conditions (heat to 80°C, then react solutions) that the rebounding effect of cooling the solution (increasing viscosity) is not very significant. This information suggests that the effect of high temperature reaction conditions dominate settling performance of the precipitate.

The cooling effect on the second reaction conditions (react solutions, then heat to 80°C) does play an important role in sedimentation. Slower sedimentation can be attributed to the higher viscosity of water and the inference that the particle properties remained relatively unchanged during the short period of exposure (15 min) at higher temperatures (54-80°C).

Although $BaSO_4$ is presumed to be essentially unaffected due to aging and agglomeration, an experiment mimicking the one performed on $BaCO_3$ is displayed in Figure 8.

BaSO₄ Settling Curves
(29ml 0.1M Ba(OH)₂, 71 ml 0.1M Na₂CO₃)
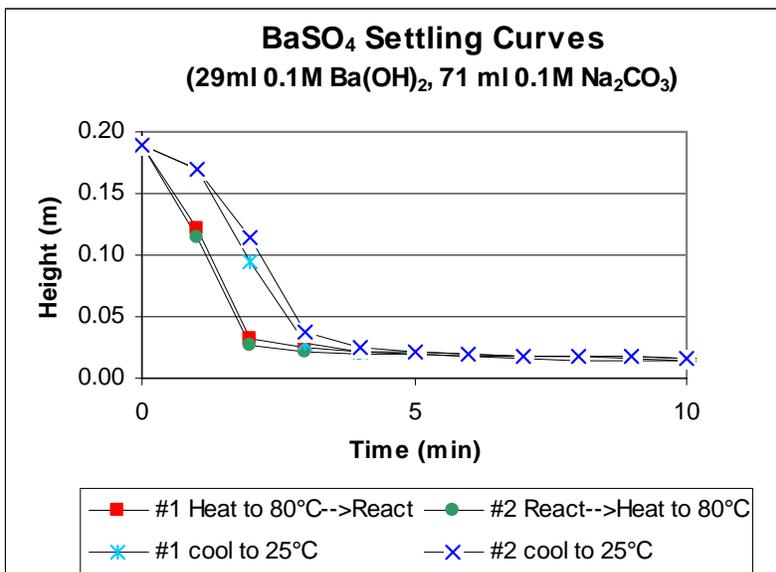
Figure 8. $BaSO_4$ settling results.

The results show that settling curves for $BaSO_4$ performed under the two precipitation reaction conditions are essentially the same. Although $BaSO_4$ responds to cooling (increasing water viscosity) as did $BaCO_3$, the response is the same regardless of the two possible prior reaction conditions.

6.4 Sedimentation: Calcium vs. Barium

So far we have seen settling curves for dilute concentrations of barium salts which amount to about 6.5 kg/m^3. This concentration value does not represent the feed inlet into a sedimentation tank. Actual inlet feeds range from 80 to 125 kg/m^3 as stated before. Dorris [4] produced laboratory lime mud to simulate industry conditions with a concentration of 100 kg/m^3 at 85°C. See Figure 9.
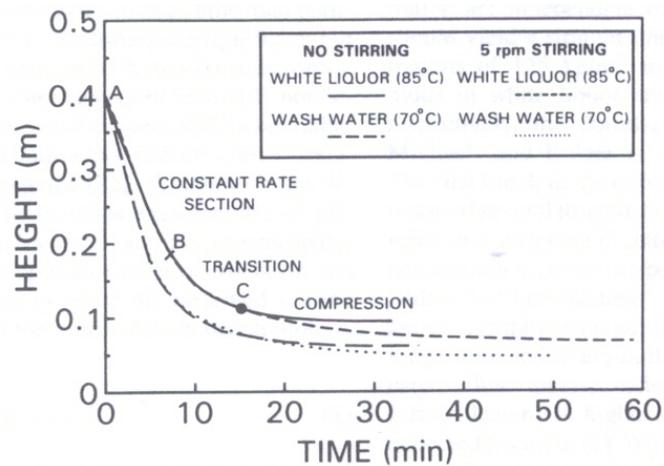
Figure 9. Settling curve for lime mud in white liquor [4].

The purpose of this study is to compare barium mud sedimentation to lime mud sedimentation. A 100 kg/m^3 slurry of 90% wt BaCO$_3$ and 10% wt BaSO$_4$ at 85°C was used to generate a setting curve. This high temperature operating condition is rather convenient since we have established using preliminary data that precipitation of barium solutions and sedimentation at high temperatures will yield optimum performance. The resulting curves are displayed in Figure 10.

23
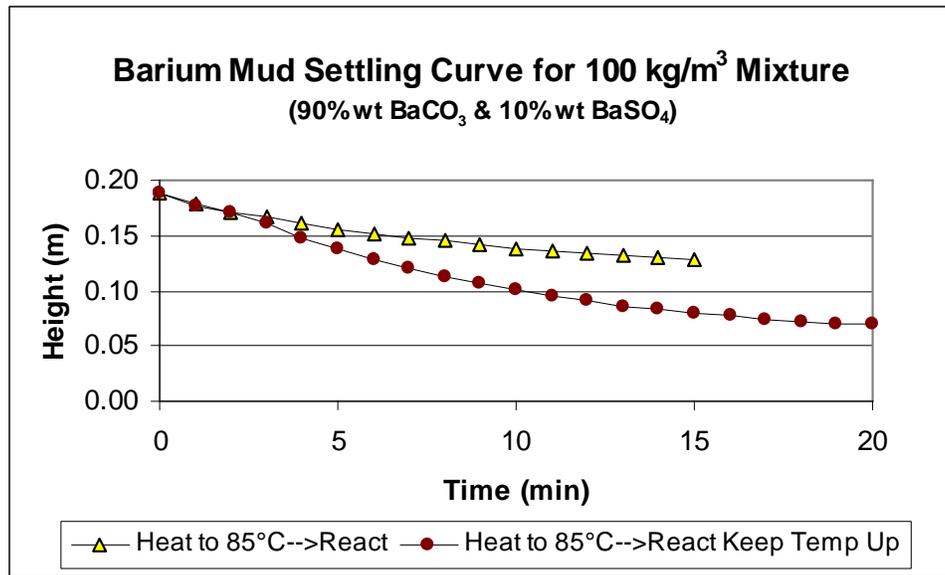
Figure 10. Barium Mud Sedimentation

The first curve shows barium mud sedimentation while cooling freely in the cylinder from 85°C to about 58°C. The second curve shows an attempt to keep the temperature constant at 85°C by placing the cylinder over a hot plate. This was difficult and unachievable with the lab equipment used. The final temperature, measured at the mid point of the cylinder, after 15 minutes was 62°C. The uneven temperature profile, due to heating the graduated cylinder over a hot plate, created natural convection currents, which aided the subsidence of the sedimentation bed structure. Industrial sedimentation tanks utilize a slow moving rake to disturb the sedimentation bed, therefore, increasing subsidence.

To compare barium mud sedimentation with that of lime mud, we need to normalize the data from Dorris's research with that of this study to a starting height of one meter and an observation time of 20 minutes. See Figure 11.
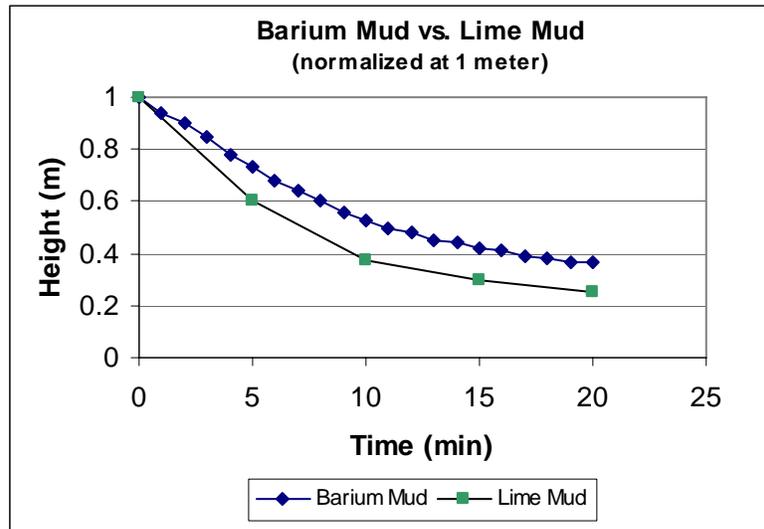
Figure 11. Barium and lime mud sedimentation comparison.

As shown above the settling behavior of barium mud approaches that of lime mud. The curve shift due to the temperature of sedimentation has been observed from data. Therefore, evidence supports the notion that the settling curve could essentially replicate that of lime mud if the temperature remained constant at 85°C during the experimental setting.

The average solids concentration within the sedimentation bed of barium mud after 20 minutes is about 22% wt. The concentration of the bottom most part of the sedimentation bed was not calculated. This would be equivalent to the underflow concentration of a sedimentation tank. As the compression layer forms regions containing lower solids concentration are near the interface of the mud blanket while those with the highest solids concentration are at the bottom due to compression by the sediments above. Therefore, it's reasonable to assume that the barium mud underflow concentration is greater than 22% wt. Typical values for lime mud underflow in sedimentation tanks are between 35% and 40% wt.

The results above show that barium mud sedimentation is comparable to that of lime mud. Barium mud sedimentation by employment of existing equipment is possible with simple manipulation of operating parameters such as temperature and barium mud feed rate.

7. Conclusions

- $BaCO_3$ and $BaSO_4$ approach full conversion (97.7% and 95.9% respectively) after a 5 to 10 second reaction at room temperature with 0.1M feed solutions ($Ba(OH)_2$, Na_2CO_3, and Na_2SO_4). Bausticizing reactions have a great advantage over that of causticizing due to the essentially full conversions as well as instantaneous reaction kinetics.

- The average particle (agglomerate) size of $BaCO_3$ decreases with age, yielding a noticeably different suspension or network when observed with the naked eye. When first reacted at 25°C, the precipitate is snowflake-like and fluffy in appearance, likely containing a significant amount of occluded water. After aging the precipitate for 7 days, it becomes more aggregated or compact, and less fluffy in appearance, likely increasing the overall specific gravity of the aggregated particle.

- $BaSO_4$ particles do not display trends which may be attributed to aging. This conclusion supports the observation of other research that $BaSO_4$ particles do not agglomerate or even age to the same extent that $BaCO_3$ does.

- Aging effects increase sedimentation performance for $BaCO_3$.

- High temperature precipitation of $BaCO_3$ will improve settling rate for any given operating temperature of sedimentation. Changes in settling performance are most likely attributed to changes in size and shape of precipitate crystal structure and agglomerates that are affected by precipitation temperature.

- $BaSO_4$ sedimentation behavior does not change due to different temperatures of precipitation performed within the limited conditions of the experiment.

- Barium mud sedimentation behavior approaches that of lime mud and can possibly be employed by existing sedimentation tanks within a pulp mill.

8. Recommendations for Future Work

- Comparison of barium mud porosity and filtration behavior to that of lime mud.
- Analyze actual crystal morphology and aggregate size of barium mud precipitated under conditions akin to that of causticizing.
- The health and ecological impact of the barium-based process should be further investigated.

9. Literature Cited

1. Green, Robert P., *Chemical Recovery in the Alkaline Pulping Processes* , Third Edition. Tappi Press. pp. 57-120. (1992).

2. Smook, Gary A., *Handbook for Pulp & Paper Technologists*, Second Edition. Angus Wilde Publications. pp. 149-150. (1992).

3. Fabien, Salvatori., Determination of Nucleation and Crystal Growth Kinetics of Barium Carbonate, Powder Technology, v 128, n 2-3, Dec 18, 2002, pp. 114-123.

4. Dorris, G.M., Physical Characterization of Hydrated Reburned Lime and Lime Mud Particles, *Journal of Paper Science*, v 19, n 6, Nov, 1993, pp.256-267.

5. Chen, Pao-Chi., Nucleation and Morphology of Barium Carbonate Crystals in a Semi-Batch Crystallizer, *Journal of Crystal Growth*, 2001, pp. 458-472

6. Nore, P.H., Batch Precipitation of Barium Carbonate, *Chemical Engineering Science*, v 48, n 17, 1993, pp. 3083-3088.

7. Aoun,M., Are Barium Sulphate Kinetics sufficiently Known for Testing Precipitation Reactor Models?, *Chemical Engineering Science*, v 51, n 10, pt A, May 1996, pp. 2449-2458.

8. Rousseaux, J.M., Aging of Precipitated Amorphous Alumina Gel, Industrial and *Engineering Chemistry Research*, v 41, n 24, Nov 27, 2002, pp. 6059-6069.

9. Grace, Thomas M., Alkaline Pulping, Pulp and Paper Manufacture, Third Edition, Vol 5: Tappi Press. pp. 574-579. (1989).

10. Tchobanoglous, George. *Wastewater Engineering: Treatment, Disposal and Reuse*, Third Edition. McGraw-Hill, Inc. pp. 229-233. (1991).

11. Perry, Robert H., *Perry's Chemical Engineers' Handbook*, Seventh Edition. McGraw-Hill. pp. 2-121. (1997).

12. Levenspiel, O., *Chemical Reaction Engineering*, Third Edition. John Wiley & Sons, Inc. pp. 15, 27, 42-44. (1999).

11. Acknowledgements